

STUDY OF CORRELATION BETWEEN WETTED FUEL FOOTPRINTS ON COMBUSTION CHAMBER WALLS AND UBHC IN ENGINE START PROCESSES

H. KIM^{1)*}, S. YOON²⁾ and M.-C. LAI¹⁾

¹⁾Department of Mechanical Engineering, Wayne State University, Detroit, MI 48202, USA

²⁾Automobile Hi-Technology Research Center, Cheonbuk National University, Cheonju-Si 561-756, Korea

(Received 6 December 2004; Revised 7 March 2005)

ABSTRACT—Unburned hydrocarbon (UBHC) emissions from gasoline engines remain a primary engineering research and development concern due to stricter emission regulations. Gasoline engines produce more UBHC emissions during cold start and warm-up than during any other stage of operation, because of insufficient fuel-air mixing, particularly in view of the additional fuel enrichment used for early starting. Impingement of fuel droplets on the cylinder wall is a major source of UBHC and a concern for oil dilution. This paper describes an experimental study that was carried out to investigate the distribution and “footprint” of fuel droplets impinging on the cylinder wall during the intake stroke under engine starting conditions. Injectors having different targeting and atomization characteristics were used in a 4-Valve engine with optical access to the intake port and combustion chamber. The spray and targeting performance were characterized using high-speed visualization and Phase Doppler Interferometry techniques. The fuel droplets impinging on the port, cylinder wall and piston top were characterized using a color imaging technique during simulated engine start-up from room temperature. Highly absorbent filter paper was placed around the circumference of the cylinder liner and on the piston top to collect fuel droplets during the intake strokes. A small amount of colored dye, which dissolves completely in gasoline, was used as the tracer. Color density on the paper, which is correlated with the amount of fuel deposited and its distribution on the cylinder wall, was measured using image analysis. The results show that by comparing the locations of the wetted footprints and their color intensities, the influence of fuel injection and engine conditions can be qualitatively and quantitatively examined. Fast FID measurements of UBHC were also performed on the engine for correlation to the mixture formation results.

KEY WORDS : Cold-start, Gasoline, Footprint, PFI, UBHC

1. INTRODUCTION

Mixture formation in the combustion chamber of an engine has a major effect on the subsequent combustion process and on undesirable emission products. Most spark-ignited (SI) gasoline engines use indirect port fuel injection (PFI) and rely on the subsequent air intake process for additional fuel-air mixing (Zhao *et al.*, 1995). Due to the large amount of unburned hydrocarbon (UBHC) generated by SI engines during the cold start and warm-up cycles, mixture formation characteristics during this period have been given special attention. This is primarily due to the fact that liquid fuel injected into the cold intake port and subsequently carried into the combustion chamber by intake charge motion is poorly vaporized during starting conditions.

Because of the low vapor pressure of fuel in this condition, extra fuel is required to produce enough vapor for successful ignition and stable flame.

The extra liquid fuel accumulates in liquid films or pools at the intake port and on the combustion chamber walls. Moreover, fuel films on the cylinder wall, crevices and piston top land may flow directly into the crankcase during the compression and expansion strokes, and create an oil dilution problem. Pool fires on the combustion chamber surfaces may also be a source of UBHC emissions at cold start. The unburned fuel vapor escaping from the inefficient pool fire combustion process or just vaporizing directly from the fuel film during the later part of the expansion stroke may enter the exhaust pipe directly and result in increased UBHC emissions.

Generally, the optimum fuel preparation conditions for low HC emissions are a well atomized spray, a spray targeted at the back surface of the intake valve head for minimum intake wall wetting, and injection timed to

*Corresponding author. e-mail: hoisankim@yahoo.com

occur during the period when the intake valve is closed (Nogi *et al.*, 1988; Zhao *et al.*, 1996).

Yang *et al.* (1993) studied the effect of port fuel injection timing and fuel droplet size on total and speciated exhaust hydrocarbon emissions. They found that compared to close valve injection (CVI), cylinder liner wetting by large fuel droplets during open valve injection (OVI) was the main reason for the hydrocarbon emission increase. OVI also results in the change in hydrocarbon species distribution in the exhaust gases and fuel losses.

Shin *et al.* (1994), and Meyer and Heywood (1997) observed the entry of liquid fuel into the cylinder and its behavior throughout the combustion cycle with a high speed CCD camera system in a optically accessible engine for a simulated cold start. They described three liquid fuel transport mechanisms into the cylinder as follows: 1) strip atomization of liquid fuel by intake flow, 2) fuel film formation on the valve surface and seat, and 3) liquid film squeezing by the closing valve. The observed in-cylinder liquid films were also categorized as follows: 1) a thick film on the valve surface and around the valve seat formed by the liquid film flow from the back of the valve and the port surfaces, 2) a thin film on the combustion chamber surfaces formed by the impingement of the droplet stream resulting from strip atomization, and 3) isolated puddles formed by drops splashed by the intake valve closing process.

Takeda *et al.* (1995) quantitatively analyzed the partitioning of fuel to intake port and cylinder wall wetting, and burned fuel and subsequent engine out hydrocarbon emissions during cold start and warm up, using a specially designed analytical engine. It was found that intake port wall wetting increased until the 300th cycle and then decreased gradually as the engine warmed up. High engine-out HC emissions were observed just after the cold engine start and decreased gradually as the engine warmed up.

Witze and Green (1997) applied imaging techniques to investigate the evolution of liquid fuel films on combustion chamber walls during a simulated cold start of a port fuel injected engine. It was found that for closed valve injection (CVI), fuel films formed on the underside of the intake valves and in the squish region between the intake valves and the cylinder wall below the intake valves. For OVI condition, fuel films formed on the underside of the exhaust valves. It was postulated that fuel films on the head near the exhaust valves are a direct source of UBHC emissions, fuel films on the cylinder wall are a source of fuel blow-by into the crankcase, and that pool fires are a source of soot.

Zughyer *et al.* (2000) visualized the liquid fuel distribution and flame propagation inside a PFI gasoline engine using various injectors and engine conditions. It

was found that most of the fuel under open-valve injection (OVI) conditions entered the cylinder as droplet mist. Images taken just before spark timing showed that a significant fraction of the fuel was still in the liquid phase. The combustion video showed that fuel transport process under both CVI and OVI strategies could be categorized into three phases. The first phase was at early cycles when most of the injected fuel ended up as liquid film on the chamber walls, with insufficiently vaporized fuel in a mixture too lean to sustain combustion and little effect on cylinder pressure. The second phase started when visible weak flame fronts appeared due to improvement in liquid evaporation process. Diffusion-controlled pool-fire processes became obvious at this phase and the in-cylinder pressure increase was significant. The third phase started when the heat of combustion evaporate most of the liquid fuel and produced an overall-rich mixture that combusted with a high speed and produced a high cylinder pressure. From the flame propagation visualization and in-cylinder pressure measurements, it was found that injectors with better dispersion and injection under open-valve conditions could provide better fuel distribution and evaporation, constituting an improved engine starting strategy. However, the UBHC emissions could be worse.

To analyze fuel droplet distribution and flow pattern in the engines and intake ports, researchers have used Laser Doppler Velocimetry (LDV), Phase Doppler Particle Analysis (PDPA) (Shin *et al.*, 1997; Meyer *et al.*, 1997; Kim *et al.*, 2004), and Laser-Induced Fluorescence (LIF) (Witze *et al.*, 1997), to characterize the source of engine-out UBHC emissions. These methodologies however, cannot directly characterize the cylinder wall wetting processes. In spite of the large number of research publications on PFI mixture formation, there has not been a direct characterization of the distribution of the fuel films or droplets impinging on the cylinder liner and piston top surfaces during the engine starting conditions.

In this paper a new Color Image Capturing Technique (CICT) developed to investigate the effects of fuel injector spray pattern, targeting, injection timing, and engine operating conditions on the distribution of wetted fuel footprints is described. The fuel footprints on the combustion chamber surfaces of a four-valve port-fuel-injection engine during an engine start were studied. Various injectors with different targeting and atomization characteristics were tested in an optically accessible engine. The fuel droplets impinging on the port wall, cylinder wall, and piston top were characterized by the CICT during a simulated engine start-up from room temperature. Fast FID measurements of UBHC were also performed on the engine to correlate the mixture formation results.

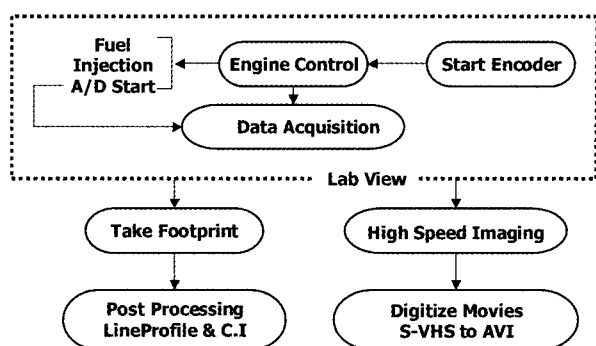
2. EXPERIMENTAL SETUP

A DOHC cylinder head was mounted on a 0.55-liter single-cylinder engine with a transparent piston crown and an extended piston (Yang *et al.*, 1993). The transparent piston crown provided a means of optical access from the bottom of the combustion chamber. A 62 mm section of transparent acrylic cylinder tube was installed between the engine head and the extended cylinder block, providing a means of optical access from the side. The acrylic cylinder section has a slightly larger bore than the piston to accommodate the filter paper during piston motion. The cylinder block and its crevice reduced the engine compression ratio from the original 9.5 to 8.2. A stationary 45-degree inclined mirror was installed on the cylinder block inside the elongated piston. The camera viewing through the inclined mirror allowed observation of both film formation around the intake valves and wall wetting on the fire deck during the intake process.

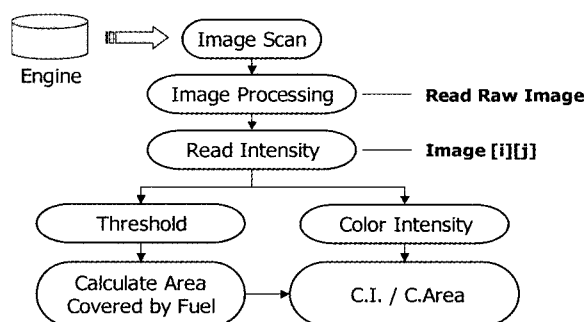
The CICT was used to characterize the liquid fuel distribution on the cylinder liner wall and piston top land. A small amount of Rodamine B was used as the dye dissolved in the fuel surrogate, which was then injected through the actual fuel supplying system. The filter paper was attached on the inside circumference of the cylinder liner and on top of piston to collect fuel films or droplets impinging on the both surfaces.

A Kodak EM-1012 EKTAPRO high-speed digital camera was used to visually record the spray in the chamber and in the intake port. The light sources utilized were a pulsed arc lamp and a continuous white light source. The results were saved on videotapes; selected sets of image frames were then digitized to create movies. In this experiment most of the fuel injection was enabled during only two cycles to optimize the visual effect. For the wall wetting visualization study inside the engine, high-speed digital video images were recorded for 4 consecutive cycles at a recording rate of up to 500 frame/sec. The engine was motored to the specified speed before fuel injection. After filling the camera memory, the engine was shut-off immediately and cooled to a pretest condition. A minimum of 1 hour was allotted to dry out all fuel inside the intake port and the combustion chamber before another recording was performed. The optical windows and acrylic liner were cleaned after each test.

The synchronization of fuel injection and data acquisition was controlled using a program written in LabVIEW. To minimize the variability in cranking speed, the engine was motored at a constant speed. Different test procedures were implemented for liquid fuel and combustion visualizations. Figure 1(a) and (b) illustrate the engine control and data acquisition flow chart. Color intensities, line profiles, and covered area were calculated



(a) Schematics of experiment - Engine control



(b) Post processing

Figure 1. Schematic of experiment and post processing.

Table 1. Engine specifications.

Specifications	Optical engine
Bore × Stroke	86 mm × 108 mm
Compression ratio	8.2
Engine speed (RPM)	220
Injection timing	OVI: 360° BTDC CVI: 102° BTDC

from the scanned images.

For this work the engine was fueled with solvent fuel surrogate. The fuel injection pressure was fixed at 380 kPa using a compressed nitrogen cylinder. The specifications of the engine and test conditions are listed in Table 1.

Table 2 summarizes the different injectors tested in this experiment. The injectors tested are all multi-hole injectors: 4 dual-streams (DS) and 1 single-stream (SS).

The injection duration was 45 ms to simulate over-enrichment conditions for engine starting. The injection duration used for the engine starting conditions is typical of the enrichment strategy used in current engines. The Sauter Mean Diameter (SMD) was measured at the maximal flux point using PDPA.

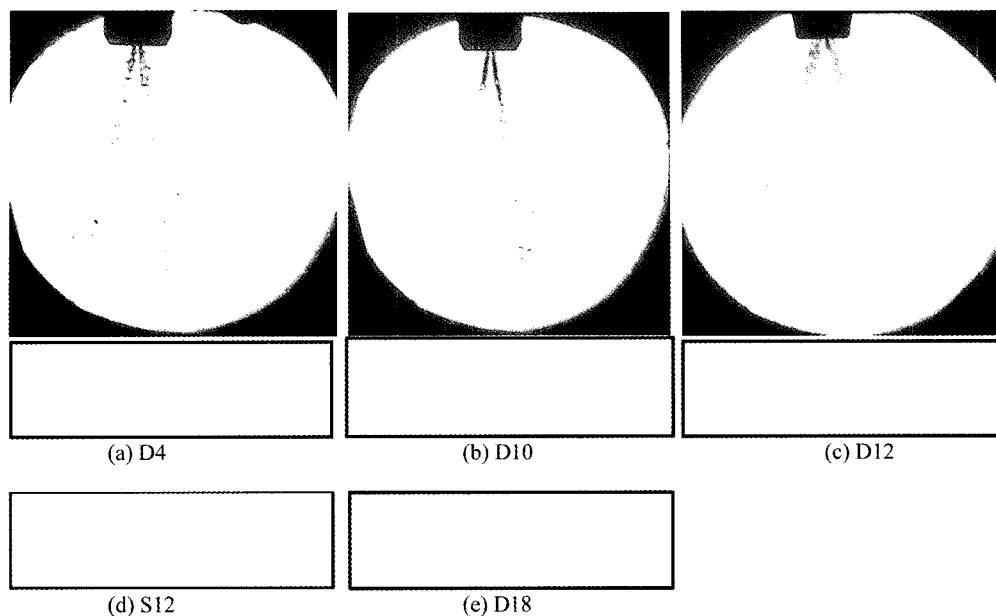


Figure 2. Typical spray behavior with footprint at 3.2 ms after one injection (Injection duration 2.5 ms).

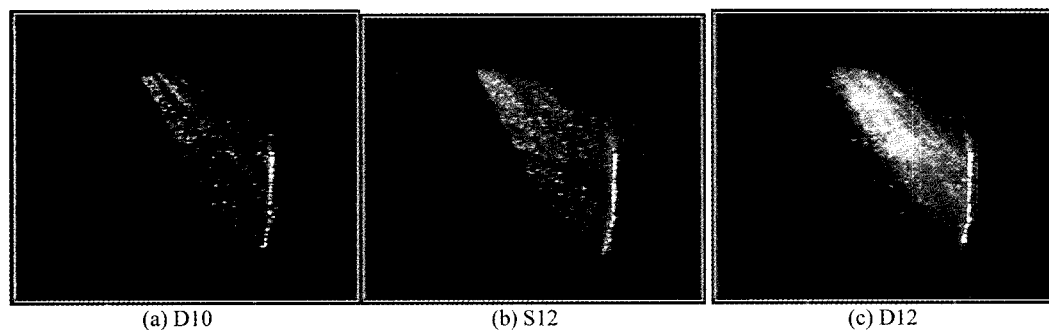


Figure 3. Spray sideview with different injectors in the intake port.

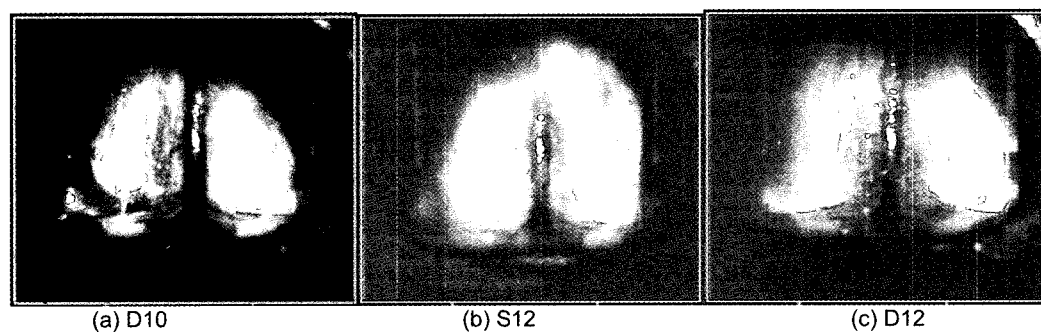


Figure 4. Spray targeting with different injectors in the intake port.

Cold start emission measurements were carried out on an engine stand (2.2 liter, 4 cylinder). The test engine was conditioned for each cold start. In each run the engine was started at room temperature and was allowed to idle

for about 15 minutes until the engine coolant temperature reached 93°C. The engine was cooled by forced convection for the subsequent cold starts.

Fast FID HFR400 was used to measure the concen-

Table 2. Injector specifications.

Injector	No. of holes	DS/SS	SMD (μm)	DV90 (μm)
D4	4	DS	75	228
D10	10	DS	56	141
S12	12	SS	53	128
D12	12	DS	61	141
D18	18	DS	72	213

tration of hydrocarbons in the exhaust stream. The hydrocarbon mass was determined from HC concentration and the molar exhaust flow. The exhaust moles were calculated from the engine airflow and the exhaust air-fuel ratio measurement.

3. RESULT AND DISCUSSION

The spray footprints and the spray backlit spray images for the injectors tested in this experiment are shown in Figure 2. The target distances, i.e., the distances from the point of injection to the paper target, were the same as those from the injector to the intake valve head. The optimal target position of the spray centroid is on the valve head, ensuring minimum intake-wall wetting. Injector D10 has a narrower stream separation angle compared to the other dual-stream injectors, D12 and D18, resulting in better targeting performance to match the intake port geometry. Spray targeting images in the intake port are shown in Figure 3 and Figure 4. Unless otherwise noted, the results shown in this paper is for Injector S12. Figure 5. is a comparative chart of injector mass flowrates at an injection duration of 45 ms.

A simple test of injection directly onto the filter paper at the target distance was carried out. It showed that the

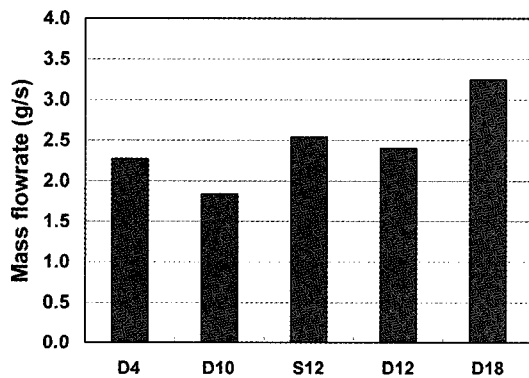


Figure 5. Mass flowrate of injectors with 45ms of injection duration: (a) D4 (b) D10 (c) S12 (c) D12 (d) D18.

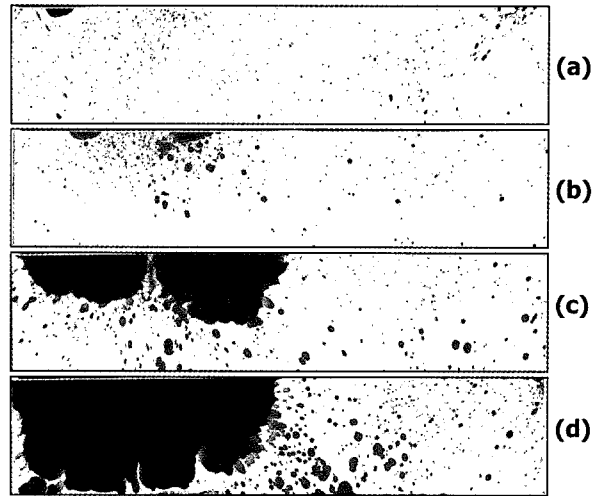


Figure 6. Cylinder liner footprints of different number of injection events of the injector D10: (a) 1 (b) 2 (c) 5 (d) 7.

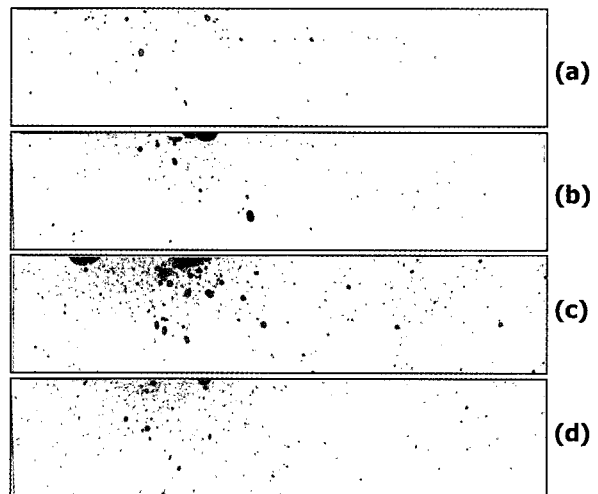


Figure 6-1. Cylinder liner footprints of different number of injection events of the injector D10: (a) 150 rpm (b) 200 rpm (c) 250 rpm (d) 300 rpm.

total color intensity is not exactly linear due to soaking of the dye into the filter paper.

At small mass of fuel injections, however, the color intensity can be used to correlate to the liquid fuel mass on the filter. Figure 6 shows the cylinder-liner footprint images with different number of enrichment injections. It clearly shows severe wall wetting from fuel film running down the liner from the intake with increasing number of enrichment injection events. The intake-valve side of the cylinder liner is the main area for fuel wetting, which is caused not only by fuel film running down the liner, but also by fuel droplets splashing from the intake valve. In order to quantify the image technique, the total color

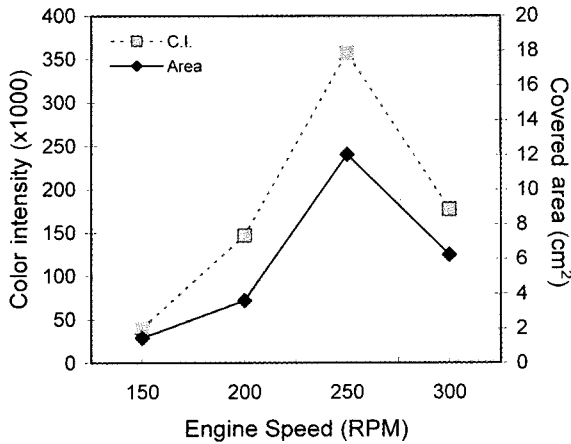


Figure 7. Effect of engine speed on color intensity and covered area of the injector D10.

intensity of the images was acquired, which is the summation of each pixel of color intensity calculated from the whole area (Cylinder Liner and Piston Top).

3.1. Effect of Engine Speed

The effects of engine cranking speed on the cylinder liner wetted footprints were also determined experimentally. Engine cranking speed increases induction air speed during the intake stroke and has a significant effect on liquid fuel trajectory and can cause fuel film stripping from the intake valve. As shown in Figure 7, increasing the engine-cranking speed from 150 to 250 rpm increases the wall wetted footprint areas and the resultant color intensity. However, at the higher engine speed of 300 rpm, the behavior changes, with less fuel wetting on the liner wall possibly due to the secondary atomization on the surface of the intake valve by the stronger induction airflow.

The CICT technique was applied to see the effects of two injection timing modes, CVI (closed valve injection, 102° BTDC) and OVI (Open valve injection, 360° BTDC), on liner wetted footprints. These timing modes are illustrated in Figure 8.

The results of a previous paper (Kim *et al.*) indicate that more severe liner wall wetting was generated on the

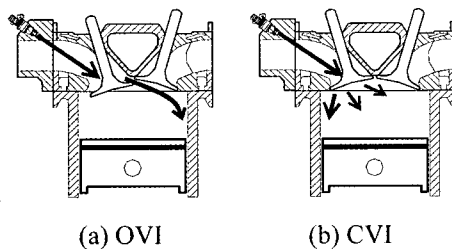


Figure 8. Comparison between OVI and CVI.

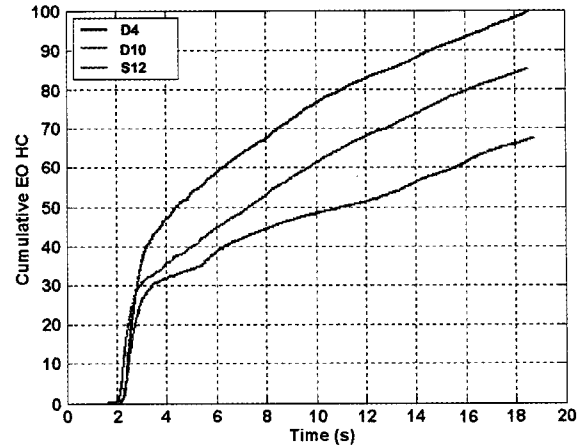


Figure 9. Engine performance comparison chart.

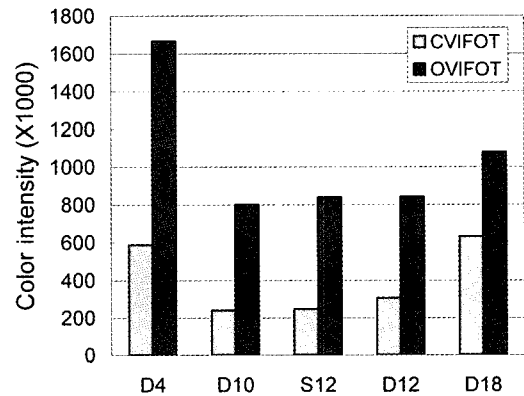


Figure 10. Color intensity on cylinder liner.

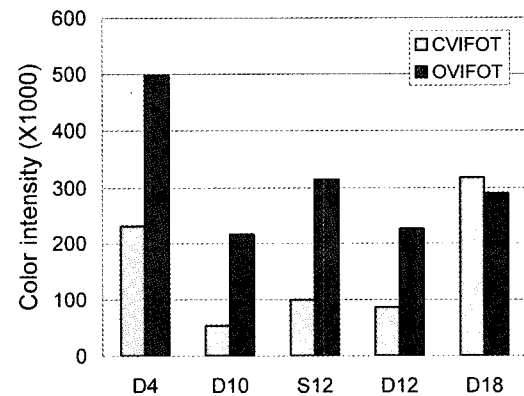


Figure 11. Color intensity on piston top.

exhaust valve side with OVI, consistent with Taketa *et al.* (1995).

3.2. Effect of Number of Holes

Using HC fast FID, engine performance was evaluated. A chart of the results is shown in Figure 9. The S12

injector with a spray angle of 30° reduced the UBHC up to 18% as compared to baseline injector with 4 holes (D4 with 19° of spray angle).

Figure 10 and Figure 11 show the color intensity results of the different injectors. The color intensity of the S12 injector is much less than that of the D4 (baseline) injector.

The liner and piston top footprints of different injectors

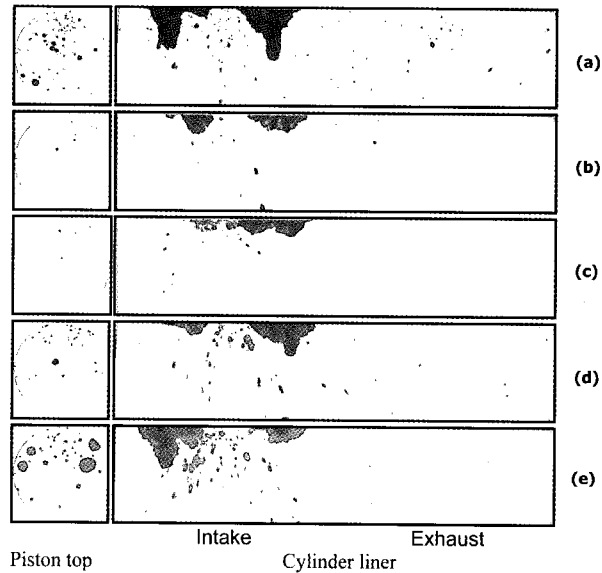


Figure 12. Piston top and cylinder liner footprint under CVI conditions with different injectors: (a) D4 (b) D10 (c) S12 (d) D12 (e) D18.

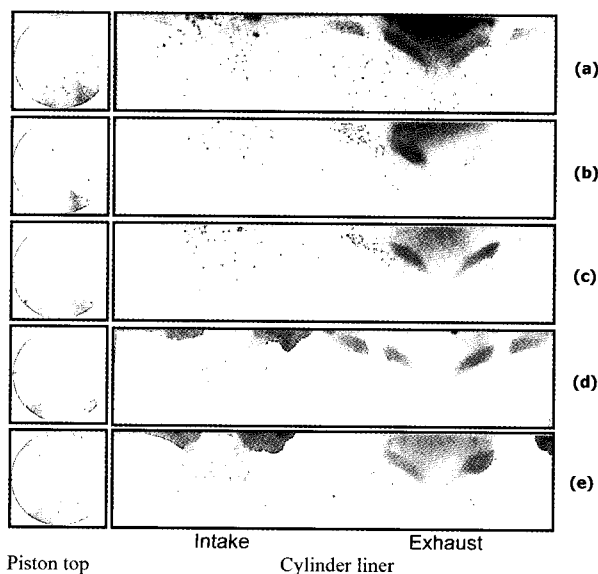


Figure 13. Piston top and cylinder liner footprint under OVI conditions with different injectors: (a) D4 (b) D10 (c) S12 (d) D12 (e) D18.

are shown in Figure 12 and Figure 13 for the CVI and OVI conditions. The CICT technique has enough sensitivity to investigate reduced UBHC during engine starting conditions.

4. CONCLUSIONS

A new measuring method, color image capturing technique (CICT) was developed to compare the effects at different conditions (engine speed, injection timing, and injector type) in an optical accessible engine. It was demonstrated that the CICT technique could be used to investigate liquid fuel distribution on the combustion chamber wall during engine starting conditions. The results of the current investigation show the following trends:

- (1) Effect of Number of Holes: The CICT technique can be used to screen injector design with regards to minimization of wall wetting. Injectors with better targeting and better dispersion can reduce the fuel-wetted footprints on the combustion chamber wall.
- (2) Effect of Injection Timing: During the cold start CVI mode fuel wall wetting is concentrated on the intake valve sides. Under OVI mode during cold start, spray droplets hit and flow down the exhaust valve faces by induction airflow.

Reducing Engine-out HC Emission: According to the HC fast FID result, emission result shows that 30% improvement of the engine-out HC emission for S12H compare with that for D4H. Color intensity result shows same trend for fuel film formation onto cylinder liner and piston top.

REFERENCES

- Kim, H., Yoon, S., and Lai, M.-C. (2003). Liquid fuel footprints on combustion chamber wall in port fuel injection engine during starting. *9th Int. Conference on Liquid Atomization and Spray Systems*, Italy.
- Kim, H., Im, K.-S., and Lai, M.-C. (2004) Pressure modulation on micro-machined port fuel injector performance. *Int. J. Automotive Technology* **5**, **1**, 9–16.
- Lee, S., *et al.* (2000). Effects of swirl and tumble on mixture preparation during cold start of a gasoline direct-injection engine. *SAE Paper No. 2000-01-1900*.
- Meyer, R. and Heywood, J. B. (1997). Liquid fuel transport mechanisms into the cylinder of a firing port-injected SI engine during start up. *SAE Paper No. 970865*.
- Nogi, T., Ohyama, Y., Yamauchi, T., and Kuroiwa, H. (1988). Mixture formation of fuel injection systems in gasoline engine. *SAE Paper No. 880558*.
- Shin, Y., Cheng, W., and Heywood, J. B. (1994). Liquid gasoline behavior in the engine cylinder of a SI engine.

- SAE Paper No. 941872.*
- Takeda, K., Yaegashi, T., Sekiguchi, K., Saito, K., and Imatake, N. (1995). Mixture preparation and HC emissions of a 4-Valve engine during cold starting and warm-up. *SAE Paper No. 950074.*
- Witze, P. O., and Green, R. M. (1997). LIF and flame emission imaging of liquid fuel films and pool fires in an SI engine during a simulated cold start. *SAE Paper No. 970866.*
- Yang, J., Kaiser, E. W., Siegel, W. O., and Anderson, R. W. (1993). Effects of port injection timing and fuel droplet size on total and speciated exhaust hydrocarbon emissions. *SAE Paper No. 930711.*
- Zhao, F. Q., Lai, M. C. and Harrington, D. L. (1995). The spray characteristics of automotive port fuel injection - a critical review. *SAE Paper No. 950506.*
- Zhao, F. Q., Yoo, J. H. and Lai, M. C. (1996). Spray targeting inside a production-type intake port of a 4-valve gasoline engine. *SAE Paper No. 960115.*
- Zughyer, J., Zhao, F. Q., Lai, M.-C., and Lee, K. (2000) A visualization study of fuel distribution and combustion inside a port-injection gasoline engine under different start conditions. *SAE Paper No. 2000-01-0242.*